Vol. 21, No. 1(2022) Alim2667
Revista Mexicana de Ingeniería Química

Effect of shrinkage and concentration basis on water diffusivity estimation and oil transfer during deep-fat frying of foods

Efecto del encogimiento y bases de cálculo en la estimación de la difusividad del agua y transferencia de aceite durante el freído por inmersión de alimentos

J. Del Rosario-Santiago[1], H. Ruiz-Espinosa[1], C.E. Ochoa-Velasco[2], A. Escobedo-Morales[1], I.I. Ruiz-López[1]*

[1] *Facultad de Ingeniería Química. Benemérita Universidad Autónoma de Puebla. Av. San Claudio y 18 Sur. Ciudad Universitaria. C.P. 72570. Puebla, Puebla. México.*

[2] *Facultad de Ciencias Químicas. Benemérita Universidad Autónoma de Puebla. Av. San Claudio y 18 Sur. Ciudad Universitaria. C.P. 72570. Puebla, Puebla. México.*

Received: November 25, 2021; Accepted: February 8, 2022

Abstract

The effect of different modeling assumptions on the estimated water diffusivities and kinetic parameters for oil transfer during deep-fat frying of foods is investigated. Modeling assumptions include the use of several common concentration units (including the water or oil mass per weight or volume of food or per weight of non-defatted or fat-free solids) to express water loss and oil absorption, leading to implicit simplifications such as constant density, constant concentration of fat-free solids or constant concentration of non-defatted solids. The proposed model was used to analyze frying experiments conducted with potato strips (9.5 mm × 9.5 mm × 80 mm) at different temperatures (160, 175, and 190 °C), where product shrinkage was followed via image analysis. The proposed model was solved under two-dimensional mass transfer and water diffusivities were estimated by the method of slopes, with and without considering the dimensional changes of the product. Mean water diffusivities were calculated in the range of 0.89×10^{-8} to 4.86×10^{-8} m^2/s for the different concentration units. How water and oil contents are expressed during frying (i.e., the concentration basis) and dimensional changes of the product have a significant effect on the estimation of water diffusivity and its severity depending on the concentration units and estimation method chosen.

Keywords: Fickian diffusion, Image processing, Shape index.

Resumen

Se investigó el efecto de diferentes consideraciones de modelación sobre la estimación de coeficientes de difusión del agua y parámetros cinéticos para la transferencia de aceite durante el freído por inmersión de alimentos. Las consideraciones incluyen el uso de varias bases de cálculo comunes para expresar la pérdida del agua y absorción de aceite (incluyendo la masa de agua o aceite por volumen o masa de alimento y por masa de sólidos desgrasados o no desgrasados), que llevan a simplificaciones implícitas de propiedades constantes como la densidad, concentración de sólidos libres de grasa o concentración de sólidos no desgrasados. El modelo propuesto se usó para analizar experimentos de freído realizados con tiras de papa (9.5 mm × 9.5 mm × 80 mm) a diferentes temperaturas (160, 175 y 190 °C), donde la evolución del encogimiento del producto se determinó vía análisis de imagen. El modelo propuesto se resolvió bajo transferencia de masa en dos dimensiones y las difusividades del agua se estimaron con el método de pendientes, con y sin considerar los cambios dimensionales del producto. Las difusividades promedio del agua se estimaron en el rango de 0.89×10^{-8} a 4.86×10^{-8} m^2/s para las diferentes unidades de concentración. La forma en la que se expresan los contenidos de agua y aceite durante el freído (i.e., la base de cálculo) y el encogimiento del producto tienen un efecto significativo en la estimación de la difusividad del agua y su severidad depende de las unidades de concentración y el método de estimación seleccionados.

Palabras clave: Difusión Fickiana, Índice de forma, Procesamiento de imagen.

* *Corresponding author. E-mail*: irving.ruiz@correo.buap.mx
https://doi.org/10.24275/rmiq/Alim2667
ISSN:1665-2738, *issn-e*: 2395-8472

1 Introduction

Deep-fat frying is one of the most important operations in the food industry, used to produce cooked products with unique flavor, color, and texture characteristics. This operation involves the simultaneous heat and mass transfer between the food material and the surrounding oil (Li *et al*., 2020), and several empirical and theoretical approaches have been applied to achieve its mathematical description with varying complexity levels. The cutting-edge modeling of water loss during frying very often includes capillarity diffusivity formulations with pressure-driven fluxes as demonstrated in selected studies (Ghaitaranpour *et al*., 2021; Gouyo *et al*., 2021); however, this approach, while rigorous, may also be difficult to apply. Thus, effective diffusivity formulations (Fickian type) are very often applied to simplify the water transfer analysis (Naghavi *et al*., 2018a,b). In this case, both numerical and analytical solutions for unsteady-state diffusion mass transfer equations have been used to describe the frying process. Moreover, diffusive models have found application in the analysis, control, simulation, and optimization of continuous industrial fryers (Nikolau, 2006; Wu *et al*., 2013).

An extensive literature review reveals that moisture diffusivity during frying has been exclusively estimated from the fit of the dimensionless water concentration versus the frying time through different analytical models. The most widespread method considers an analytical solution developed under an equilibrium boundary (Dirichlet or first-type boundary) (Movahhed and Chernabon, 2019; Topete-Betancourt *et al*., 2020); however, some authors have used a third-type or Robin boundary condition to consider an important contribution of external convection to overall mass transfer rate (Kose and Dogan, 2017). In most cases, regression methods produce a single diffusivity value for the fitted frying data interval. Besides, some authors have attempted to study the variability of water diffusivity during frying using an explicit time-dependent function with monotonically increasing or decreasing diffusivity values (Moyano and Berna, 2002). In other cases, a numerical solution of the frying model has been used to allow the estimation of variable diffusivity expressions (Chen and Moreira, 1997). However, this strategy has its shortcomings as the chosen diffusivity model forces a predefined, unvalidated diffusivity behavior, possibly masking the effect of other phenomena on diffusion coefficients, such as shrinkage. On the other hand, most of the oil gained by food remains confined to the surface region immediately after frying (Li *et al*., 2020; Touffet *et al*., 2020); thus, most studies dealing with the mathematical description of oil uptake during frying use empirical models, such as exponential and Peleg equations or artificial neural networks, among others (Ayustaningwarno *et al*., 2020; Jeong *et al*., 2021); which, in some cases, have also been applied to describe water loss.

One of the most evident physical changes in food matrices when dehydrated is they get shrink, mainly due to the removed water volume. Shrinkage has a major effect on the estimation of mass transport properties, as has been demonstrated in drying and osmotic dehydration operations (González-Pérez *et al*., 2019; Estévez-Sánchez *et al*., 2021); yet, product shrinkage is neglected in most frying studies even if it has been proven significant (Roshani *et al*., 2021), with just one study incorporating the effect of dimensional changes of food for estimating water diffusivity (Baik and Mittal, 2005). An additional challenge to compare and discuss water diffusivity values or oil transfer properties during frying of foodstuffs is how moisture loss and oil uptake data are reported (that is, the concentration basis), leading to different implicit modeling assumptions about the variability of some food properties, whose effects of estimated parameters remain unknown. Therefore, this study aims to evaluate the mass transfer of water and oil during the frying of shrinking foods. To achieve this purpose the following topics are covered: (i) derive the relationships between different concentration units used to express moisture loss and oil uptake data and discuss their role in the resulting assumptions for mass transfer models, (ii) develop a simple method for the estimation of variable water diffusion coefficients of shrinking food matrices, (iii) evaluate morphometric changes of the product along dominant mass transfer directions by image analysis techniques and the mathematical description of resulting data and (iv) analyze the diffusivity behavior obtained under different concentration bases.

2 Methods and materials

2.1 *Basic definitions*

Water loss and oil uptake during frying can be characterized in terms of several process variables having different bases (for example, per weight or volume of food or per weight of non-defatted or fat-free solids). In this section, mathematical relationships between them are presented, allowing their interconversion and comparison. In the following expressions, the product (p) is constituted by fat-free solids (s), water (w) and oil (o). The mass (m) of fat-free solids, water, and oil per food volume (V), that is, the volumetric concentration (c) is ($j = w, o, s$)

$$c_j = \frac{m_j}{V} \tag{1}$$

Similarly, the mass of fat-free solids, water, and oil per food weight, that is, the mass fraction (X) is given by

$$X_j = \frac{m_j}{m_p} = \frac{m_j}{m_s + m_w + m_o} \tag{2}$$

with

$$X_w + X_o + X_s = 1 \tag{3}$$

Water and oil contents can be also expressed as their mass ratio concerning a given component. The water- or oil-to-fat-free solids mass ratio (Y) is defined as ($k = w, o$)

$$Y_k = \frac{m_k}{m_s} \tag{4}$$

while the mass ratio of a given component ($j = w, o, s$) to the non-defatted product solids (Z) is

$$Z_j = \frac{m_j}{m_s + m_o} \tag{5}$$

Variables X_k and Z_k ($k = w, o$) are often referred to as the water/oil content in wet and dry bases, respectively. The volumetric concentration of water and oil ($k = w, o$) can be expressed in terms of the quantities X, Y and Z as

$$c_k = \rho X_k = c_s Y_k = c_{os} Z_k \tag{6}$$

Here, ρ is the apparent food density (the ratio between the weight of food and the volume it occupies), c_s is the volumetric concentration of fat-free solids [the ratio between the mass of fat-free solids and the food volume as defined by Eq. (1) for $j = s$] and c_{os} is the volumetric concentration of non-defatted solids (the ratio between the mass of non-defatted solids and the food volume). Eq. (4) can be used to obtain the relationships between these properties as follows:

$$\begin{aligned} c_{os} &= \frac{m_o + m_s}{V} = \frac{m_s Y_o + m_s}{V} = \frac{m_s}{V}(Y_o + 1) \\ &= c_s(Y_o + 1) \end{aligned} \tag{7}$$

$$\begin{aligned} \rho &= \frac{m_o + m_w + m_s}{V} = \frac{m_s Y_w + m_s Y_o + m_s}{V} \\ &= c_s(1 + Y_w + Y_o) = \frac{c_{os}(1 + Y_w + Y_o)}{1 + Y_o} \end{aligned} \tag{8}$$

On the other hand, the relationships between variables X, Y and Z can be developed by combining Eqs. (2) to (5) ($j = w, o, s$)

$$\begin{aligned} Z_j &= \frac{m_j}{m_o + m_s} = \frac{m_p X_j}{m_p X_o + m_p X_s} = \frac{X_j}{X_o + X_s} \\ &= \frac{X_j}{1 - X_w} \end{aligned} \tag{9}$$

$$Z_j = \frac{X_j}{X_o + X_s} = \frac{X_s Y_j}{X_s Y_o + X_s Y_s} = \frac{Y_j}{Y_o + Y_s} = \frac{Y_j}{Y_o + 1} \tag{10}$$

$$\begin{aligned} X_j &= \frac{m_j}{m_s + m_w + m_o} = \frac{m_s Y_j}{m_s + m_s Y_w + m_s Y_o} \\ &= \frac{Y_j}{1 + Y_w + Y_o} \end{aligned} \tag{11}$$

$$\begin{aligned} X_j &= \frac{m_j}{m_s + m_w + m_o} = \frac{(m_s + m_o) Z_j}{m_s + (m_s + m_o) Z_w + m_o} \\ &= \frac{Z_j}{1 + Z_w} \end{aligned} \tag{12}$$

$$X_S = 1 - X_w - X_o = 1 - \frac{Z_w}{1 + Z_w} - \frac{Z_o}{1 + Z_w} = \frac{1 - Z_o}{1 + Z_w} \tag{13}$$

$$\begin{aligned} Y_j &= \frac{m_j}{m_s} = \frac{m_p X_j}{m_p X_s} = \frac{X_j}{X_s} = \frac{(m_s + m_o) Z_j}{(m_s + m_o) Z_s} = \frac{Z_j}{Z_s} \\ &= \frac{Z_j}{1 - Z_o} \end{aligned} \tag{14}$$

Frying curves can be also monitored in terms of the water loss or oil uptake per initial mass of product (γ) which is defined as ($k = w, o$)

$$\gamma_k = \frac{m_k - m_{k0}}{m_{p0}} = \frac{Y_k - Y_{k0}}{1 + Y_{w0} + Y_{o0}} \tag{15}$$

where the subscripts p and 0 refer to product and initial state, respectively. Finally, the dimensionless water loss or oil uptake (Ψ) is given by the expression

$(k = w, o)$

$$\Psi_k = \frac{m_k - m_{ke}}{m_{k0} - m_{ke}} = \frac{Y_k - Y_{ke}}{Y_{k0} - Y_{ke}} \tag{16}$$

The subscript e denotes an equilibrium value in above equation.

2.2 Water transfer model

Unsteady-state mass transfer of water within the product can be described by a Fickian diffusion model

$$\frac{\partial c_w}{\partial t} = \nabla \cdot [D_w \nabla (c_w)], \quad \text{in } V \tag{17}$$

where t is the time, and c_w and D_w represent the volumetric concentration and apparent diffusivity of water, respectively. Eq. (17) can be expressed in dimensionless form by introducing the variables

$$u = \frac{c_w - c_{we}}{c_{w0} - c_{we}} \tag{18}$$

$$\tau = \frac{D_w t}{L^2} \tag{19}$$

where u is the dimensionless water concentration, L is the characteristic length for diffusion, and τ is the mass Fourier number. Notice that Eq. (19) implies that both L and D_w do not have temporal variation; they are essentially constant. However, we can retain the temporal variation in L and D_w by using the following modified mass Fourier number

$$\theta = \int_0^t \frac{D_w}{L^2}\, dt \tag{20}$$

Eq. (20) implies that L does not have spatial variation, but it could change its value over time; albeit not necessarily an explicit time function. In the same way as L, let us consider that D_w is not a space-dependent variable, but it could change during the process (Estévez-Sánchez *et al*., 2021). Neglecting the spatial variation of L and D_w is a reasonable assumption as moisture content as well as product size are determined from experimental measurements involving the whole product. Eq. (20) allows to express Eq. (17) as

$$\frac{\partial u_w}{\partial t} = \nabla \cdot [\nabla (u_w)], \quad \text{in } V \tag{21}$$

If both L and D_w are constant, then θ becomes τ in the above expression. Eq. (21) is often solved by using a proper boundary condition at the product surface under a uniform water distribution in the product at the beginning of the process ($u_w = 1$ at $\tau = 0$ in V). The analytical or numerical solutions to Eq. (21) for the cases where both L and D_w change or not during the process are identical under a negligible external resistance to mass transfer ($u_w = 0$ at $\tau > 0$ on A) as the boundary condition does not depend on both L and D_w. The difference between these two cases is how the original time scale is recovered. If L and D_w are constant then $\theta = \tau$ and time can be analytically obtained from Eq. (19); however, when L and D_w retain their temporal variation the following initial value problem must be solved

$$\frac{d\theta}{dt} = \frac{D_w}{L^2}, \text{ subjected to } \theta(t = 0) = 0 \tag{22}$$

The volume-averaged solution of Eq. (21), hereafter referred to as $\langle u_w \rangle$, is a function of the mass Fourier number, that is, $\langle u_w \rangle = f(\tau) = f(\theta)$. The time-derivative of the averaged solution is

$$\frac{d\langle u_w \rangle}{d\theta} = \frac{d\langle u_w \rangle}{d\tau} = \frac{L^2}{D_w} \frac{d\langle u_w \rangle}{dt} \tag{23}$$

Eq. (23) provides a way to estimate diffusion coefficients as

$$D_w = L^2 \frac{d\langle u_w \rangle / dt}{d\langle u_w \rangle / d\tau} = L^2 \frac{d\langle u_w \rangle / dt}{d\langle u_w \rangle / d\theta} \tag{24}$$

The use of Eq. (24) to estimate diffusion coefficients is known as the method of slopes (MOS). It is widely used in convective drying and is valid whether L and D_w retain or not their temporal variation (Tlatelpa-Becerro *et al*., 2020; Estévez-Sánchez *et al*., 2021). Here, $d\langle u_w \rangle / dt$ is evaluated from the numerical differentiation of experimental data while $d\langle u_w \rangle / d\theta = d\langle u_w \rangle / d\tau$ is calculated from an available analytical or numerical solution.

2.3 Proposed estimation method for water diffusivities

As shown in Section 2.1, the water and oil contents during frying can be reported in several ways, each one can be used to obtain a general diffusion model such as that presented in Eq. (21). However, a different assumption will be implicitly used in each case. For example, if the product density (ρ) is constant then u in Eq. (18) can be expressed in terms of the mass fraction of water (X_w) instead of volumetric concentration (c_w). Similarly, if c_s and c_{os} are constant then u can be written in terms of variables Y and Z, respectively. For

simplicity, let us consider the notation $u(y)$ indicates that u is calculated from $y = c_w, X_w, Y_w$ or Z_w, that is,

$$u(y) = \frac{y_w - y_{we}}{y_{w0} - y_{we}} \tag{25}$$

Thus, water diffusivities can be estimated from Eq. (24) under different assumptions by simply using a proper definition for u. Please notice that $u(\gamma_w) = \Psi_w = u(Y_w)$; thus, both $u(\gamma_w)$ and Ψ_w are not considered in subsequent analyses.

A major drawback to applying Eq. (24) in the estimation of water diffusion coefficients during frying is the natural dispersion of experimental data (unlike drying, each point in frying curves involves a different sample due to the destructive nature of the fat content analysis). This variability is more notorious in the evaluation of $d\langle u\rangle/dt$; numerical differentiation amplifies error. This difficulty can be overcome by previously fitting experimental data to a suitable model as shown by Gómez-de la Cruz *et al*. (2020) for the convective drying process. In this case, the following models are proposed for the preliminary fit of experimental frying curves

$$Y_w = (Y_{w0} - Y_{we})e^{-k_w t^{n_w}} + Y_{we} \tag{26}$$

$$Y_o = Y_{oe}\left(1 - e^{-k_o t^{n_o}}\right) \tag{27}$$

where $k_w, k_o, n_w, n_o, Y_{we}$, and Y_{oe} are adjustable parameters. Eqs. (26) and (27) are based on the Page's model, a popular drying equation including a shape factor n to account for deviations from the first-order behavior while k adjusts the drying rate. On the other hand, Y_{we} and Y_{oe} determine the final dehydration and oil absorption levels of food. In drying processes, the Page's model is presented in terms of the moisture content on dry basis as the food solids constitute an invariable basis of calculation (they remain constant during drying). Thus, Y is selected over c, X and Z as the fat-free solids are constant during frying. The following procedure is proposed to obtain the six parameters k_k, n_k and Y_{ke} simultaneously fitting the eight curves of c_k, Y_k, X_k and $Z_k (k = w, o)$ for each frying temperature:

1. Propose an initial estimation of parameters k_k, n_k and Y_{ke} $(k = w, o)$.

2. Evaluate Eqs. (26) and (27) to obtain $Y_{k,mod}$ $(k = w, o)$.

3. Calculate $c_{k,mod}$, $X_{k,mod}$ and $Z_{k,mod}$ from $Y_{k,mod}$ $(k = w, o)$ and definitions given in Eqs. (6)-(14).

4. The following sum of absolute errors (SAE) is proposed as the fitness quality index

$$SAE = \sum_{y=c,Y,X,Z}\left(\sum_{k=w,o}\left(\sum_{i=1}^{N}\left|y_{ki,exp} - y_{ki,mod}\right|\right)\right) \tag{28}$$

Parameters k_k, n_k and Y_{ke} can be then used to obtain a smoothed behavior of $(d\langle u(y_k)\rangle/dt)_{exp}$ $(k = w, o)$.

The theoretical $(d\langle u(y_k)\rangle/d\theta)_{mod}$ $(k = w, o)$ can be evaluated from an analytical or numerical solution. In this case, the following two-dimensional mass transfer model in an infinite square prism was applied (Olguín-Rojas *et al*., 2019)

$$\langle u(y_k)\rangle = \left(\frac{8}{\pi^2}\sum_{n=1}^{\infty}\frac{1}{(2n-1)^2}\exp\left(-\frac{(2n-1)^2\pi^2\theta}{4}\right)\right)^2 \tag{29}$$

Water diffusivities were then estimated by applying Eq. (24) updating L with its instantaneous value. Moreover, mass diffusivities were also estimated under the rigid solid assumption, this is, $L = L_0$. An averaged diffusion coefficient was evaluated for each frying temperature as

$$\langle D_w(y)\rangle = \frac{\int_{Y_{w0}}^{Y_{we}} D_w(y)\, dY_w}{\int_{Y_{w0}}^{Y_{we}} dY_w} \tag{30}$$

In Eq. (30), the notation $D_w(y)$ indicates diffusivity values were estimated from y data ($y = c_w, X_w, Y_w$ or Z_w).

2.4 *Experimental validation*

2.4.1 *Frying experiments*

Fresh, well-graded potatoes (*Solanum tuberosum* L. cv. Alpha), free from physical or microbiological damage, were purchased from a local market (Puebla, Puebla, México) and fried the same day. Potatoes were washed, dried with a cloth, skinned with a manual peeler, and cut into slices with a French fry cutter (9.5 mm-square openings) to produce strips that were further cut to the desired length (80 mm). On average, 8 regular slices were obtained from each tuber. Potato strips were blanched in hot water (85 °C) for 3.5 min using a product-to-water mass ratio of 1:20. The resulting blanched samples were dried with a paper towel to eliminate the water excess.

Deep frying experiments were conducted in an electrical fryer (T-Fal, Family Pro Fryer, Canada)

with commercial soybean oil. Before frying, the oil was preheated at the desired frying temperature (160, 175 or 190 °C) for 15 min. The oil-to-potato mass ratio was set to 50:1 to prevent changes in frying temperature. Two sets of experiments were conducted to obtain the frying behavior of potato strips. Water loss and oil uptake kinetics were obtained from the first experimental set. In this case, slices were removed from the oil at predefined frying times until reaching a final moisture content of about 0.7 kg water/kg product (between 180 and 300 s). Before moisture and oil contents analyses in both groups of experiments, samples were drained after frying and placed between paper towels for 5 min to allowed them to cool while the excess of oil adhered to the product surface was eliminated. All experiments were carried out in duplicate and the oil was replaced after processing samples for a single frying curve. The second experiment set was conducted by frying potato strips at different time intervals (20, 40, 60, 90, 120 and 150 s) to obtain their shrinkage and deformation behavior by image analysis. A single transversal slice (perpendicular to the longest dimension) of about 1 mm-thick was cut with a sharp blade from the central part of the strip. Digital images of the resulting slices were immediately taken. The remaining product portions were analyzed for their moisture and oil contents.

2.4.2 *Image analysis*

Image analysis is a powerful technique used to extract different morphometric and quality descriptors of food products during dehydration processes. In this study, the shrinkage of potato strips during frying was analyzed according to the methodology developed by Ortiz-García-Carrasco *et al*. (2015). Figure 1 shows the applied image analysis steps for a representative potato strip fried at 160 °C for 150 s. Briefly, transversal potato slices were placed on a blue paper sheet along with a metal washer (1.22 cm-diameter), and their digital images were acquired (Coolpix L810, Nikon Corp., Japan) (Figure 1a). A digital camera was positioned with its sightline normal to the product surface for taking the pictures. Color information obtained from pictures was transformed to the CIELAB color space and grouped in four clusters (Figure 1b) for image segmentation and background extraction (Figure 1c). Product images without background were transformed to gray-scale format to obtain their boundary coordinates (600 points) (Figure 1d).

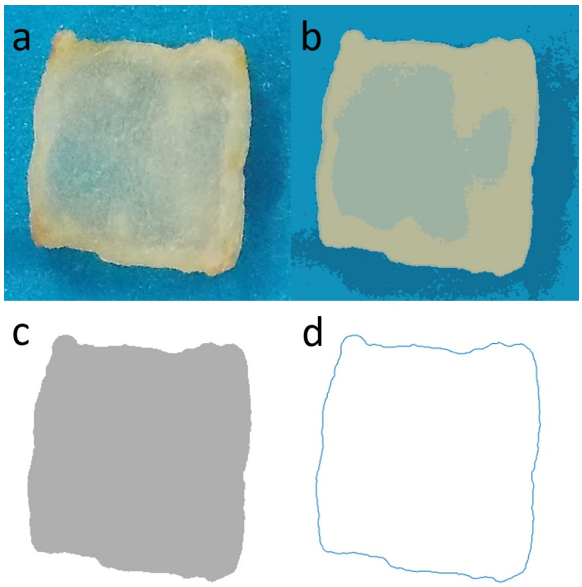

Figure 1. Image preprocessing steps to obtain product contours: (a) original image of transversal slice, (b) color reduction to four clusters, (c) gray-scale image after background removal and (d) contour extraction (600 points). Image shows a potato strip fried at 160 °C for 150 s.

Five transversal potato slices were analyzed for each process time-frying temperature combination, resulting in 95 total images. Relevant characteristics of product shrinkage and deformation at selected sampling times were obtained by averaging product contours to produce a single shape as proposed by Ortiz-García-Carrasco *et al*. (2015). This procedure is exemplified in Figure 2 for potato strips fried at 160 °C for 90 s, where the strip contours (Figure 2a) are aligned by using a point set registration method based on the iterated closest point algorithm (Figure 2b). Cross-sectional area (A) and roundness index (I_r) were evaluated from averaged strip contours (Figure 2c) and further related with their water content. The roundness index was evaluated as:

$$I_r = \frac{\text{cross-sectional area of product}}{\text{area of the minimum circle enclosing product contour}} \tag{31}$$

Sample volume was calculated from its cross-sectional area and length allowing the estimation of apparent density (ρ), the concentration of non-defatted solids (c_{os}) and the concentration of fat-free solids (c_s) with Eqs. (7) and (8).

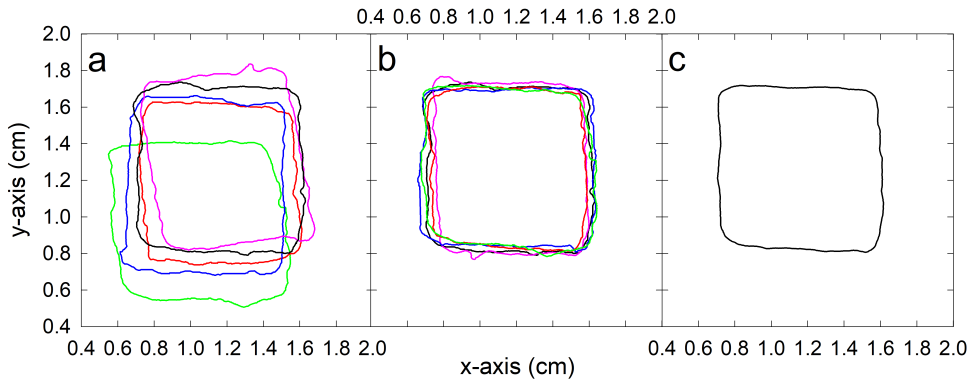

Figure 2. Extraction of representative morphological characteristics of fried potato strips: (a) original potato slice contours, (b) optimal alignment with point-set registration method (black contour is fixed in space while the rest is moved) and (c) averaged contour. Contours were obtained from potato strips fried at 160 °C for 90 s.

2.4.3 *Chemical analyses*

The moisture content of blanched and fried potato strips was determined by oven-drying the samples at 105 °C until constant mass weight. The mass of water (m_w) in the product was considered as the weight difference between the initial (m_p) and final (m_{os}) states. Dried strips were further subjected to Soxhlet extraction for 4 h with petroleum ether at its boiling point to determine their oil content. The ether extract was dried after extraction to eliminate the solvent. The weight of the dried ether extract was considered as the mass of oil in strips (m_o). The mass of free-fat solids was calculated as the difference between the mass of dried strips before extraction (m_{os}) and the mass of oil (m_o). Data for m_w, m_o and m_s were further used to calculate X_k, Y_k and Z_k (for $k = w, o$) with Eqs. (2), (4) and (5).

2.5 *Comparison with other methods for estimating variable diffusion coefficients*

A common technique to evaluate variable diffusion coefficients during drying is to solve an analytical mass transfer model for the Fourier number from certain dimensionless moisture content (Ramachandran *et al.*, 2018). This procedure is applied with the Fourier number definition given in Eq. (19). An instantaneous water diffusivity is then solved from τ with t and L. Moreover, a variable L can be used with this method to consider product shrinkage in the estimation of mass diffusivities. This procedure was applied by Rice and Gamble (1989) to obtain variable water diffusion coefficients during frying of non-shrinking potato chips and is further used to estimate water diffusivities under the investigated concentration units. This method was implemented by providing $\langle u(y_w)\rangle$ in Eq. (29) and solving for θ (which is relabeled as τ). Then, D_w is calculated from t and L and with Eq. (19).

2.6 *Statistical analyses*

Numerical procedures, nonlinear regression based on ordinary least squares and statistical analyses were performed with the Matlab software and its Statistic Toolbox 7.3 (Matlab R2010a, MathWorks Inc., Natick, MA, USA). Plots in this study were prepared with the SigmaPlot 12.5 software (Systat Software Inc., San Jose, CA, USA). The difference between predicted (y_{mod}) and experimental (y_{exp}) responses was quantified with the R^2 statistic and the mean relative deviation (MRD) (González-López *et al.*, 2021):

$$MRD = 100 \sum_{i=1}^{N} \frac{\left| \frac{y_{i,mod} - y_{i,exp}}{y_{i,exp}} \right|}{N} \tag{32}$$

where N is the number of available data. This index can be adapted to quantify the instantaneous experimental variability (IEV) within replicated frying kinetics (those conducted at a single temperature) as follows:

$$IEV = 100 \sum_{i=1}^{r} \frac{\left| \frac{y_{exp,i} - \bar{y}_i}{\bar{y}_i} \right|}{r} \tag{33}$$

where y_{exp} and $\bar{y}$ denote an arbitrary experimental response and its average value per frying time (for

$y = c_w, X_w, Y_w$ or Z_w), respectively, while r denotes the number of available replicates. The IEV can be averaged along the frying experiment to obtain a representative measure of the total experimental variability (TEV) as

$$TEV = \frac{\sum_{j=1}^{N} IEV_j}{N} \tag{34}$$

3 Results and discussion

3.1 Shrinkage characteristics of fried potato strips

Morphometric characteristics of the cross-section of fried potato strips were successfully appraised with the proposed methodology (Figure 1 and 2). The shrinkage and deformation behavior was unique for each sample, but they displayed similarities, as shown in Figure 2a for potato strips fried at 160 °C for 90 s. Therefore, the representative description of product shape from averaged profiles is desirable (Figure 3). Figure 4a shows the evolution of normalized area and roundness of averaged profiles (Figure 3) from fried potato strips as a function of the water content (kg water/kg fat-free solids). Initial values of these variables were determined by image analysis as 91.2 mm^2 and 0.564, respectively. These values were slightly different than those expected from the size of chipper openings (9.5 mm), corresponding to 90.3 mm^2 and 0.637 (this roundness value was estimated by assuming a square for the cross-sectional area), respectively. The initial sample perimeter estimated by image analysis was 3.84 cm on average; thus, the total available surface for mass transfer is about 32.5 cm^2 with square faces of potato strips contributing to less than the 6% of this value and allowing to neglect the longitudinal water loss and oil uptake (an assumption made during the model development). The cross-sectional area and its roundness showed a significant decrease with moisture content ($p < 0.05$). It was found that potato strips suffered a similar size reduction and shape change through the process for comparable dehydration levels regardless of frying temperature. A comparable behavior was previously reported by Ziaiifar *et al.* (2010) during the frying of potato strips (8 mm × 8 mm × 60 mm, 140-185 °C). The roundness index allows detecting product deformation as its value does not change for samples shrinking without altering its geometrical

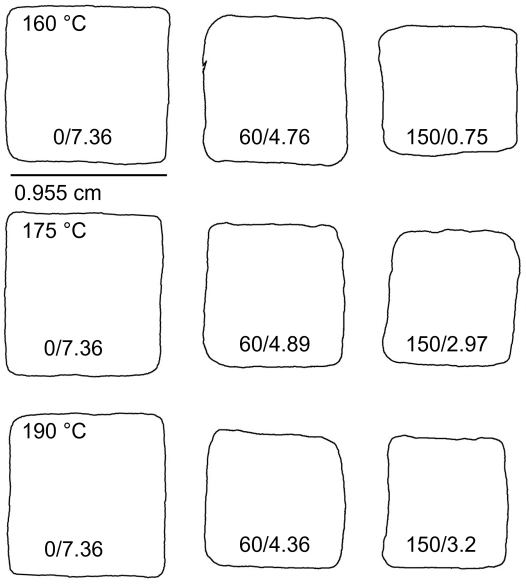

Figure 3. Morphological evolution of potato strips fried at different temperatures. Inner numbers represent the elapsed frying time (s)/water content (kg water/kg fat-free solids).

proportions. In this case, the roundness of potato strips decreased from its starting value reaching a constant behavior ($I_r/I_{r0} \approx 0.91$) when the water content is lower than 6 kg water/kg fat-free solids. Potato strips deformation was mainly perceived as the development of surface rugosity and slating of those faces that were originally parallel, as shown in Figures 1, 2 and 3 for several frying conditions. On the other hand, the cross-sectional area of potato strips reduced up ≈ 40% of its starting value ($A/A_0 \approx 0.6$). Thus, the characteristic length for diffusion is reduced by about 25% at the end of frying ($L/L_0 \approx 0.75$ by assuming a square cross-section). The following zero-intercept models were identified (bold values in parentheses represent the 95% confidence intervals) to describe the change of roundness (gray line in Figure 4a) and cross-sectional area (black line in Figure 4a) of the potato strips as a function of their water content, providing a satisfactory fit of experimental data:

$$\frac{I}{I_{r0}} - 1 = -0.20(\pm 0.04)\left(1 - \frac{Y_w}{Y_{w0}}\right) \tag{35}$$
$$\left(R^2 = 0.83, MRD = 3.20\%\right)$$

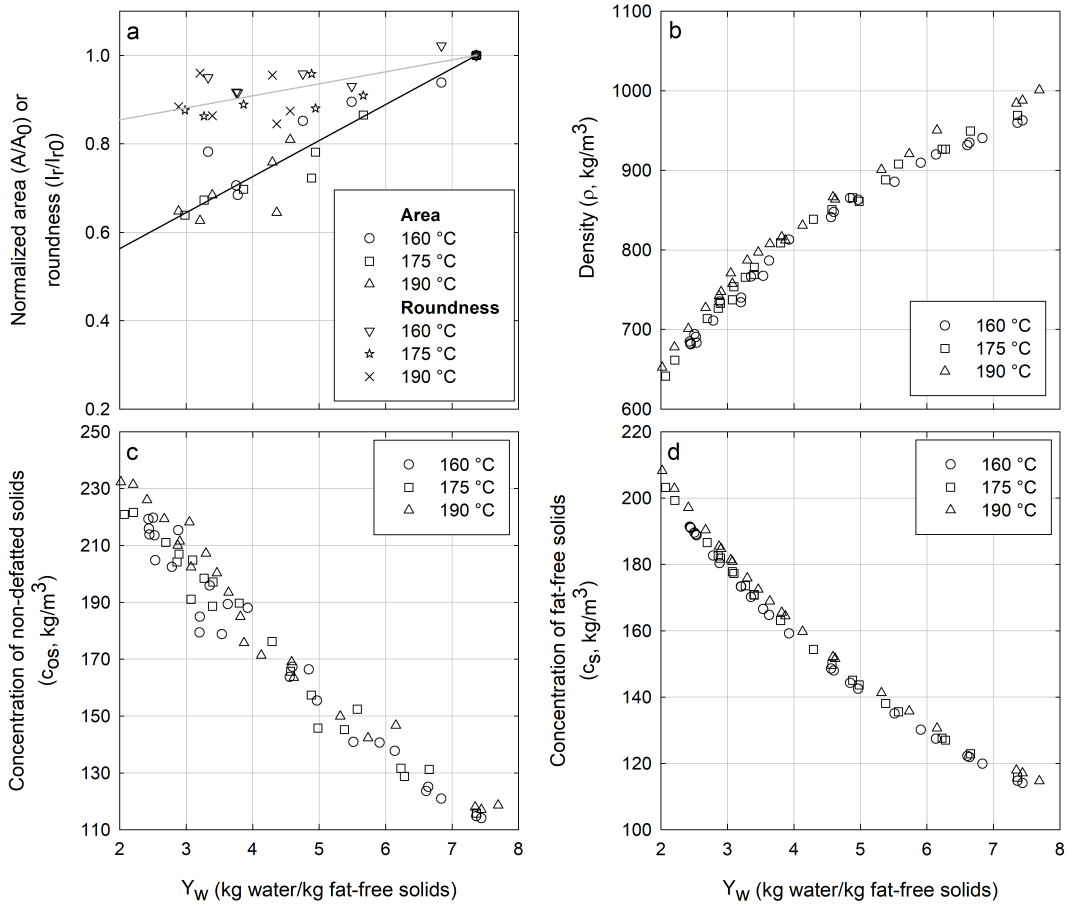

Figure 4. Evolution of shrinkage characteristics of fried potato strips. (a) Normalized area and roundness, (b) density, (c) concentration of non-defatted solids, and (d) concentration of fat-free solids.

$$\left(\frac{L}{L_0}\right)^2 - 1 = \frac{A}{A_0} - 1 = -0.60(\pm 0.05)\left(1 - \frac{Y_w}{Y_{w0}}\right) \quad (36)$$
$$\left(R^2 = 0.97, MRD = 3.89\%\right)$$

The cross-sectional area model was further used to implement product shrinkage during the estimation of mass transfer properties. The evolution of product density (ρ), concentration on non-defatted solids (c_{os}) and concentration of fat-free solids (c_s) are presented in Figures 4b-4d. These properties were in the ranges of $632 \leq \rho \leq 1001$, $115 \leq c_{os} \leq 231$ and $115 \leq c_s \leq 209$ kg/m^3. Product density reduced during frying up to about 65% of its initial value (Figure 4b), whereas c_{os} doubled and c_s increased by 80% (Figures 4c and 4d, respectively). The increase of c_{os} and c_s during frying is expected in a product having an important size reduction, while the reduction of product density occurs when mass is removed from the product faster than the observed volume decrease, leading to a more porous product (Ziaiifar *et al*., 2010). Thus, besides considering product shrinkage, the frying model should also include the variability of these properties to allow for a reliable estimation of mass diffusivities. Krokida *et al*. (2000a) reported a similar behavior for apparent density during frying of potato strips where this property reduced from a starting value of about 1030 kg/m^3 to 666 kg/m^3 at 170 °C and 583 kg/m^3 at 190 °C.

3.2 Water loss and oil uptake behavior

Experimental and fitted water loss and oil uptake kinetics for the various concentration units are shown

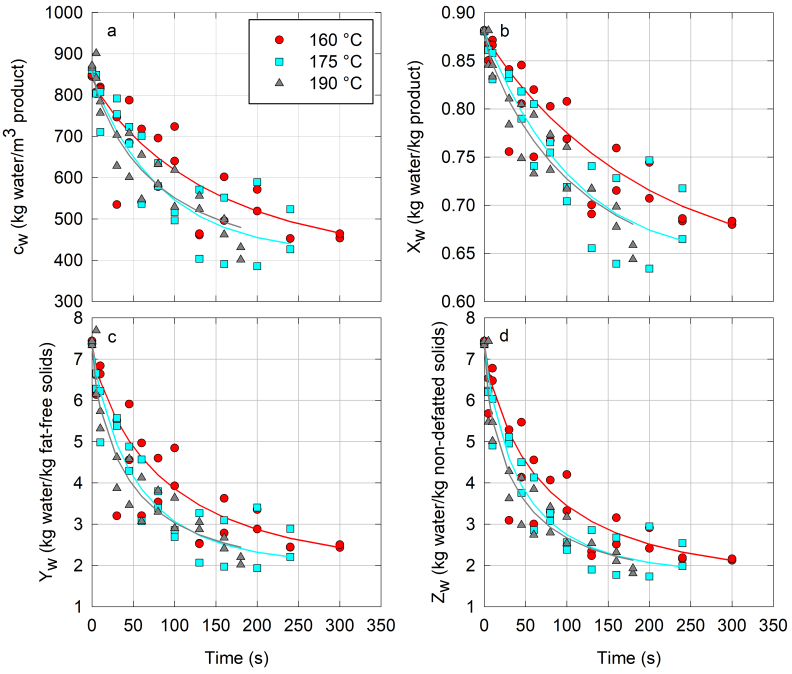

Figure 5. Experimental and fitted dehydration curves of fried potato strips in terms of different concentration units. (a) volumetric concentration of water, (b) mass fraction of water, (c) water-to-fat-free solids ratio, and (d) water-to-non-defatted solids ratio.

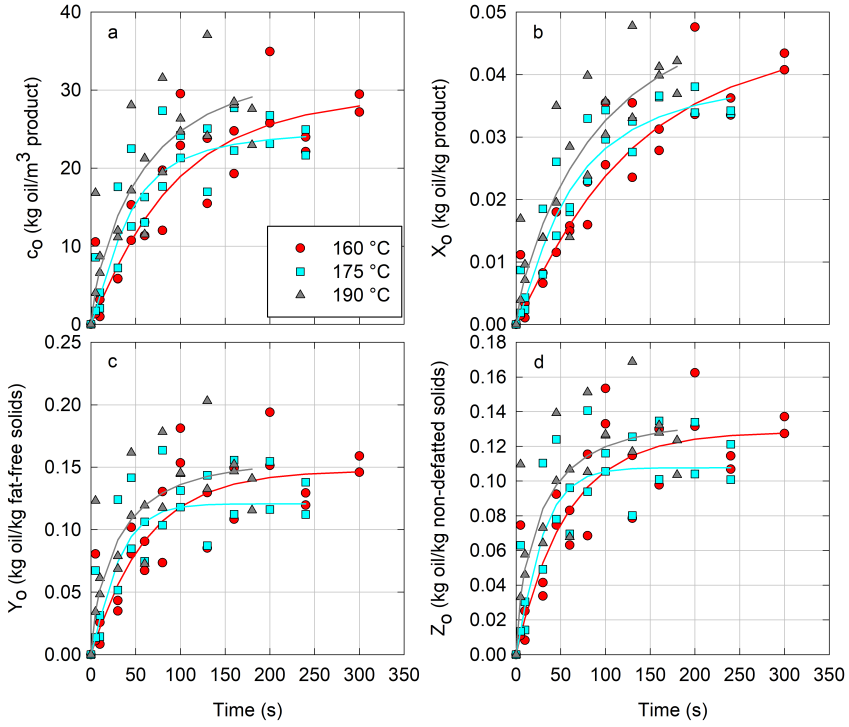

Figure 6. Experimental and fitted oil absorption curves of fried potato strips in terms of different concentration units. (a) volumetric concentration of oil, (b) mass fraction of oil, (c) oil-to-fat-free solids ratio, and (d) oil-to-non-defatted solids ratio.

Table 1. Indices and parameters describing water loss and oil uptake during frying of potato strips under different concentration units.[1]

T (°C)	Substance	*TEV* (%)				Fitted parameter[2]			*MRD* (%)				R^2				*SAE*
		c_k	X_k	Y_k	Z_k	$Y_{ke}\times10^1$	$k_k\times10^2$	n_k	c_k	X_k	Y_k	Z_k	c_k	X_k	Y_k	Z_k	
160	$k = w$	4.78	1.92	8.67	9	19.4	3.14	0.76	7.4	2.75	13.7	12.7	0.78	0.82	0.82	0.86	26.1
	k = o	20.3	20.7	21.4	20.2	1.47	1.5	1.02	25.2	22.6	29.2	27.2	0.85	0.89	0.75	0.77	
175	$k = w$	7.02	2.84	11.3	10.4	20.2	3.7	0.82	7.75	3.21	12.7	12.3	0.85	0.84	0.89	0.93	22.1
	k = o	21.6	18.6	25.5	23.7	1.21	1.87	1.16	21.6	20.4	24.5	22.8	0.85	0.91	0.72	0.75	
190	$k = w$	4.29	1.84	7.63	8.25	19.6	7.04	0.68	5.31	2.3	9.22	9.86	0.92	0.91	0.92	0.93	17.5
	k = o	18.8	20	17.2	15.7	1.54	7.93	7.15	19.3	20.3	18.5	16.8	0.77	0.83	0.66	0.69	

[1]Mass of water ($k = w$) or oil ($k = o$) per food volume (c_w), per food weight (X_w), per weight of fat-free solids (Y_w) and per weight of non-defatted solids (Z_w).
[2]Y_{ke} has units of kg diffusing substance/kg fat-free solids, k_k has units of s^{-n_k} and n_k is dimensionless.

in Figures 5 and 6, respectively. A qualitative difference between the plots occurs during the first 50 s, where plots based on the water/oil-to-fat-free solids or non-defatted solids mass ratios (Y or Z, respectively) exhibit a steeper slope than those using volumetric concentration or mass fraction of oil and water (c or X, respectively), allowing to observe a well-marked trend for the equilibrium values. Initial water content values were determined as c_{w0} = 840 kg water/m^3 product, X_{w0} = 0.88 kg water/kg product, Y_{w0} = 7.36 kg water/kg fat-free solids and Z_{w0} = 7.36 kg water/kg non-defatted solids (Y_{w0} and Z_{w0} values coincide because fat-free and non-defatted solids are the same at the start of the frying process). The indices and parameters describing the water loss and oil uptake during frying of potato strips are presented in Table 1. The concentration basis was found to significantly affect the TEV of dehydration curves ($p < 0.05$), with lower values observed when X_w is used (1.84 to 2.84%) followed by c_w (4.29 to 7.02%), while responses Y_w and Z_w produced similar experimental dispersions, from 7.63 to 11.3% and from 8.25 to 10.4%, respectively. A higher TEV was found in oil uptake curves in comparison with their dehydration counterparts ($p < 0.05$); however, no significant differences were observed between the concentration units, with $TEVs$ ranging from 15.7 to 25.5%. Unlike drying kinetics, points at each frying time in Figures 5 and 6 come from different samples, because the analysis is destructive, and every specimen may proceed from different tubers (having different properties such as initial moisture content or density); besides no sample shrinks and deforms in the same way when processed as seen in Figure 2. Therefore, the uniqueness of samples affects their mass transfer characteristics and produces a high experimental dispersion, as seen in other operations involving destructive analyses, such as osmotic dehydration (González-Pérez *et al*., 2019). The SAE lumps the variability of all concentration units (c, X, Y, and Z) in a single value, allowing the estimation of a unique set of model parameters for Eqs. (26) and (27) describing all dehydration or oil absorption curves (Y_{ke}, k_k, and n_k for $k = w, o$) at each frying temperature. This index varied between 17.5 and 26.1, allowing a good reproduction of experimental results, with individual MRD and R^2 values in the ranges of 5.31-12.7% and 0.78-0.93 for water loss and 16.8-29.2% and 0.66-0.91 for oil uptake. The MRD values follow the previously discussed trend for the TEV behavior; however, MRD indices are higher on average with an absolute difference of 2%. These results are expected as MRD indices should approach TEV ones when the model produces the best achievable fit of experimental data. The estimated water content at equilibrium (Y_{we}) ranged from 1.9 to 2.0 kg water/kg fat-free solids, while final oil contents (Y_{oe}) were between 0.12 and 0.15 kg oil/kg fat-free solids (Table 1). The corresponding ranges for the other concentration units were $370 \leq c_{we} \leq 400$ kg water/m^3 product, $24 \leq c_{oe} \leq 30$ kg oil/m^3 product, $0.63 \leq X_{we} \leq 0.64$ kg water/kg product, $0.038 \leq X_{oe} \leq 0.050$ kg oil/kg product, $1.7 \leq Z_{we} \leq 1.8$ kg water/kg non-defatted solids and $0.11 \leq Z_{oe} \leq 0.13$ kg oil/kg non-defatted solids, as estimated from Y_{we} and Y_{oe} with definitions given in Section 2.1. Current results are comparable to those reported by Krokida *et al*. (2000b), with final water and oil contents of $0.37 \leq Z_{we} \leq 0.88$ kg water/kg non-defatted solids ($0.27 \leq X_{we} \leq 0.47$ kg water/kg non-defatted solids) and $0.19 \leq Z_{oe} \leq 0.34$ kg water/kg non-defatted solids ($0.10 \leq X_{oe} \leq 0.19$ kg water/kg non-defatted solids), respectively. These values were obtained after a 10 min frying (150, 170 and 190 °C) for blanched (70 °C, 10 min) potato strips (10 mm × 10 mm × 40 mm) with an initial water content of Z_{w0} = 3.9 kg water/kg non-defatted solids (X_{w0} = 0.80 kg water/kg product).

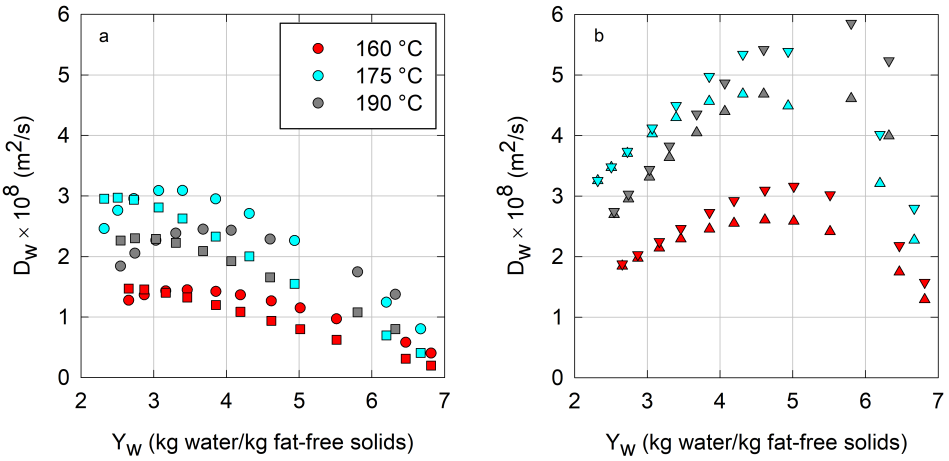

Figure 7. Water diffusivity behavior estimated with the MOS in shrinkable fried potato strips under the different concentration units. (a) circle: estimated from c_w (no simplifications), square: estimated from X_w (constant density), and (b) upside triangle: estimated from Y_w (constant concentration of fat-free solids), downside triangle: estimated from Z_w (constant concentration of non-defatted solids).

Table 2. Averaged water diffusivities estimated under different concentration bases during frying of potato strips (values×10^8 m^2/s).

T (°C)	Water concentration units[1]			
	c_w	X_w	Y_w	Z_w
160	1.12	0.89	2.25	2.63
175	2.42	1.92	4.15	4.71
190	2.14	1.73	4.2	4.86

[1]Mass of water per food volume (c_w), per food weight (X_w), per weight of fat-free solids (Y_w) and per weight of non-defatted solids (Z_w).

3.3 Effect of concentration basis on diffusivity values

A comparison of the estimated water diffusivity behavior obtained with the MOS under the tested concentration units (c_w, X_w, Y_w, and Z_w) and shrinking solid assumption is shown in Figure 7. In all cases, the proposed method predicts a gradual increase in water diffusivity values as moisture content reduces from its initial state; however, the duration of this stage is variable. The gradual increase in water mobility is very likely related to a preheating period of the product. Estimated values decrease after reaching their maximum for $D_w(c_w)$ (circles in Figure 7a), $D_w(Y_w)$ (upside triangles in Figure 7b) and $D_w(Z_w)$ (downside triangles in Figure 7b) but remain nearly constant as frying proceeds for $D_w(X_w)$ (squares in Figure 7a). The decreasing in water diffusivity values at the end of frying may be as well related to crust development. Averaged diffusivities during frying are summarized in Table 2. Mean water diffusivities were calculated in the ranges of $1.12 \leq \langle D_w(c_w)\rangle \leq 2.42$, $0.89 \leq \langle D_w(X_w)\rangle \leq 1.92$, $2.25 \leq \langle D_w(Y_w)\rangle \leq 4.20$ and $2.63 \leq \langle D_w(Z_w)\rangle \leq 4.86$ ($\times 10^{-8}$ m^2/s). The assumptions of a constant concentration of both fat-free solids (c_s) or non-defatted solids (c_{os}) led to an overestimation of diffusivity values in about 41 to 101% for c_s constant and from 55 to 135% for c_{os} constant when compared to those estimated without simplifications (estimated from c_w or c_o data), while the assumption of constant product density (ρ) led to underestimated diffusion coefficients (in about 19 to 55%). Besides producing an erroneous evaluation of frying time and water content in food which may lead to its undesirable quality changes, underestimation/overestimation of diffusion coefficients may also cause the prediction of higher evaporation rates and higher energy inputs to compensate the oil temperature reduction when the mass transfer is coupled to heat transfer equations describing both oil and product phases, impairing an effective design of the operation and their control systems. Therefore, it is important the development of reliable estimation methods for mass transfer properties. A comparison of fitted frying kinetics for water at 160 °C presented in dimensionless form is

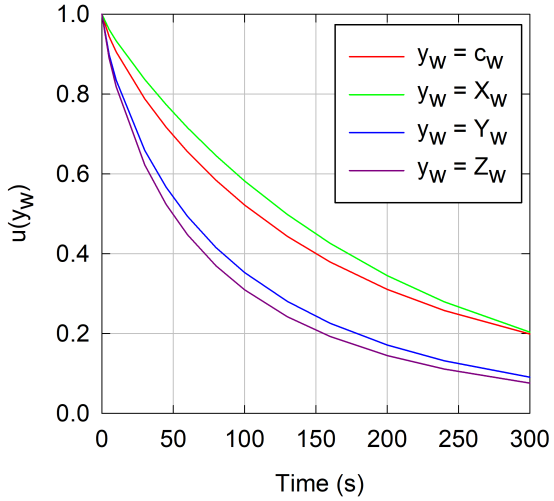

Figure 8. Comparison of dimensionless water contents during frying of potato strips estimated from different concentration units (160 °C).

given in Figure 8. According to this figure and Table 2, the faster the curve reaches the equilibrium, the lower the estimated diffusion coefficients are. The curves follow the order $u(Z_w) > u(Y_w) > u(c_w) > u(X_w)$ from the fastest to the slowest. This result does not depend on the rate constant or equilibrium values for each curve, because all kinetics share the same parameters (k_w, n_w and Y_{we}) presented in Table 1, but on formulas in Section 2.1 to change the concentration basis.

Regarding the evolution of water diffusivity behavior, several authors have fitted diffusion models with time-dependent diffusivity functions to experimental data (Moyano and Berna, 2002). In this case, monotonically increasing functions are physically inconsistent, as water diffusivity increases without bound as frying proceeds. On other hand, for monotonically decreasing functions, the problem is that water diffusivity reaches its maximum value at the start of frying without reflecting the preheating stage of samples. Therefore, the use of predefined diffusivity equations is not a good strategy to study the real evolution of this mass transfer property.

Water diffusivity values are in the same magnitude orders as those reported by other authors; however, caution should be taken when comparing these data because of the different concentration units. Besides, important differences may exist between pretreatment methods that could affect the mass transfer properties of the product. For example, Rice and Gamble (1989) determined $D_w(X_w)$ values in the ranges of 0.82-1.55 $\times$ 10^{-8} m^2/s and 1.03-1.50 $\times$ 10^{-8} m^2/s during frying of potato chips (1.5 mm slices) at 165 and 185 °C, respectively. Yildiz *et al*. (2007) determined $D_w(Z_w)$ in the ranges of 0.92-1.82 $\times$ 10^{-8} m^2/s during frying of potato strips (8.5 mm $\times$ 8.5 mm $\times$ 70 mm, 150-190 °C). Moyano and Berna *et al*. (2002) determined constant $D_w(Z_w)$ values in the ranges of 0.41-0.67 $\times$ 10^{-8} m^2/s during frying of blanched (8 min, 75 °C) and dried (60 °C up to a moisture content of 0.6 kg water/kg product) potato strips (7 mm $\times$ 7 mm $\times$ 70 mm, 150-190 °C). Naghavi *et al*. (2018a,b) reported Dw(Zw) in the range of 3.7-4.7 $\times$ 10^{-8} m^2/s during frying (170 °C; the oil-to-potato mass ratio of 40:1) of coated (1-2% w/v aqueous solutions of sodium alginate, carrageenan or Arabic gum; 2 min; room temperature) and uncoated potato strips (1.2 cm $\times$ 1.2 cm $\times$ 4 cm).

3.4 Effect of shrinkage on diffusivity values

The effect of neglecting product shrinkage on water diffusivity estimated by the MOS can be seen in Figure 9 and Table 3. An important overestimation of water diffusivity (> 170% under the explored experimental conditions) occurs when dimensional changes of the product are neglected in process modeling, independently of the used concentration basis. This effect is well-documented in other dehydration operations such as convective drying and osmotic dehydration (Ortiz-García-Carrasco *et al*., 2015; González-Pérez *et al*., 2019), and its intensity depends on the shrinkage degree of the processed material. Studies incorporating the effect of product shrinkage on water diffusivity estimation in fried foods are near to non-existent, and the existing few have resorted to regression approaches to fit moisture-dependent diffusivity expressions from water content in the form of Z_w data and a Fickian diffusion model (Baik and Mittal, 2005). However, no results have been presented regarding the overestimation degree of mass diffusivities when shrinkage is not considered in the frying model.

3.5 Effect of estimation method on water diffusivity values

A comparison of water diffusivity values obtained at 175 °C with the MOS method and by solving the analytical solution (27) under both the shrinking and rigid solid assumptions is presented in Figure 9 and Table 3. The MOS overestimates diffusivities when shrinkage is neglected under all concentration

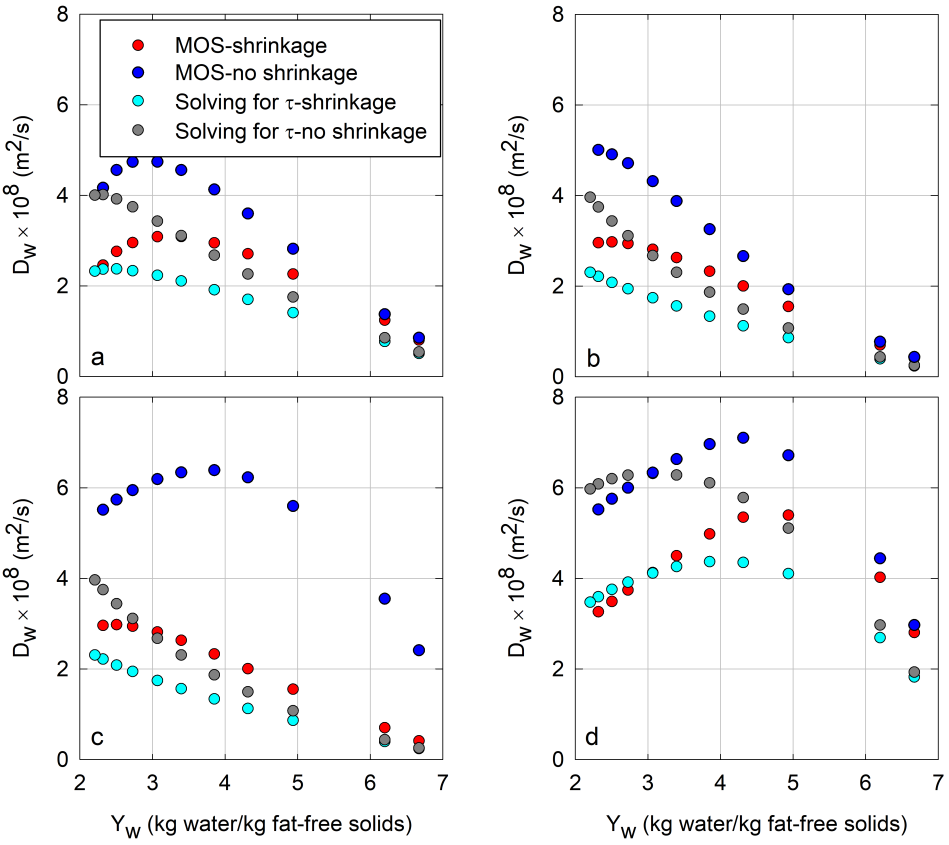

Figure 9. Effect of shrinkage and estimation method on water diffusivity behavior during frying of potato strips at 175 °C. (a) estimated from c_w (no simplifications), (b) estimated from X_w (constant density), (c) estimated from Y_w (constant concentration of fat-free solids), and (d) estimated from Z_w (constant concentration of non-defatted solids).

Table 3. Effect of shrinkage and model solution on averaged water diffusivities during frying of potato strips at 175 °C (values×10^8 m^2/s).

Method	Assumptions used in model development			Water concentration units[2]			
	Fourier number	Shrinkage	Variable D_w	c_w	X_w	Y_w	Z_w
MOS (proposed)	$\theta = \int(Dw/L)dt$	Yes	Yes	2.42	1.92	4.15	4.71
MOS (proposed)	$\theta = \int(Dw/L)dt$	No, $L = L_0$	Yes	7.53 (211)	6.45 (236)	11.6 (180)	12.7 (170)
Solving for τ	$\tau = D_w t/L$	Yes[1]	Yes[1]	1.21 (-50)	3.24 (69)	1.64 (-61)	3.99 (-15)
Solving for τ	$\tau = D_w t/L$	No, $L = L_0$	Yes[1]	1.74 (-28)	4.43 (131)	2.30 (-44)	5.43 (15)

[1]Variability of L or D_w is forced in Fourier number. [2]Mass of water per food volume (c_w), per food weight (X_w), per weight of fat-free solids (Y_w) and per weight of non-defatted solids (Z_w). Numbers in parentheses represent the relative deviation (%) with respect to MOS with shrinkage and variable diffusivity.

units (second row in Table 3); however, no simple generalizations on the expected overestimation or underestimation of mass diffusivities can be given for the method relying on solving for τ in Eq. (29), as results vary widely between concentration units (third and fourth rows in Table 3). Moreover, caution is required when comparing these data. Let us consider results for Z (Figure 9d, column Z_w in Table 3). In this case, the method based on solving for τ in mass transfer equation underestimates/overestimates

average water diffusivity by 15% when shrinkage is considered/neglected in calculations (cyan/gray circles in Figure 9d, third and fourth rows in column Z_w), when compared with the corresponding MOS (red circles in Figure 9d, first row in column Z_w). The MOS by itself, when using Z_w data (red circles in Figure 9d, first row in column Z_w in Table 3), overestimates water diffusivity by 95% in comparison with the MOS based on c_w data (red circles in Figure 9d, first row in column c_w). Nevertheless, even whether the average diffusivities are comparable, the predicted evolution of water diffusivity could be different (see for example the predicted duration of the preheating period in Figures 9a and 9d). Thus, this method must be used with caution because it estimates variable diffusivities in a shrinking product from a starting mass transfer model developed under the assumption of a constant diffusivity in a rigid solid.

Conclusions

Image analysis was proven a valuable method to extract the morphometric characteristics of fried foods for mass transfer modeling purposes. How oil and water contents are expressed in fried products significatively affects both the observed dispersion in experimental dehydration curves and the estimated water diffusivities. The use of moisture content on dry basis, the most popular way to express them, leads to overestimated water diffusivity values, ranging from 55 to 135%, in comparison with those estimated without simplifications, regardless if shrinkage is considered in the model. Therefore, it was demonstrated that special attention is required when comparing mass diffusivities in fried products from different studies. Moreover, current results may apply to the effective design of frying processes and their control systems as underestimated/overestimated diffusivities may result in the prediction of higher evaporation rates and higher energy inputs to compensate the oil temperature reduction and the erroneous evaluation of frying time and water content in food, factors impairing the development of high-quality fried foods.

Acknowledgments

Jisel del Rosario Santiago acknowledges her doctoral scholarship from CONACYT (Grant number 633571). Dr. Irving Israel Ruiz López wishes to thank the CONACYT for providing financial support through projects CF19-194782 and 100474666-VIEP2021.

Nomenclature

A	cross-sectional area of potato strips (m^2)
c	concentration (kg/ m^3 product)
D	effective diffusivity (m^2/s)
I_r	roundness index (dimensionless)
IEV	instantaneous experimental variability (%)
k	rate parameter for frying curves (s^{-n})
L	characteristic length for diffusion (m)
m	mass (kg)
MRD	mean relative deviation (%)
n	shape parameter for frying curves (dimensionless)
N	number of available observations
r	number of available replicates
t	time (s)
$u, \langle u \rangle$	dimensionless concentration: local and volume-averaged, respectively
T	temperature (°C)
TEV	total experimental variability (%)
V	product volume (m^3 product)
X	mass fraction (kg/kg product)
y	auxiliary variable denoting either c, X, Y, or Z
Y	water- or oil-to-fat-free solids mass ratio (kg/kg fat-free solids)
Z	water- or oil-to-non-defatted solids mass ratio (kg/kg non-defatted solids)

Greek symbols

γ	mass change per mass of initial product (kg/kg product)
ρ	apparent product density (kg product/m^3 product)
θ	mass Fourier number considering the temporal variation of D and L
τ	mass Fourier number under constant both D and L
Ψ	dimensionless water loss or oil uptake

Subscripts

0	denotes the initial value
e	denotes the equilibrium value
exp	denotes an experimental result
mod	denotes a predicted result
o	denotes the oil
os	denotes the non-defatted solids
p	denotes the product

s non-fat solids
w denotes the water

References

Ayustaningwarno, F., Verkerk, R., Fogliano, V. and Dekker, M. (2020). The pivotal role of moisture content in the kinetic modeling of the quality attributes of vacuum fried chips. *Innovative Food Science and Emerging Technologies 59*, 102251. https://doi.org/10.1016/j.ifset.2019.102251

Baik, O.-D. and Mittal, G.S. (2005). Heat and moisture transfer and shrinkage simulation of deep-fat tofu frying. *Food Research International 38*, 183-191. https://doi.org/10.1016/j.foodres.2004.10.003

Chen, Y. and Moreira, R.G. (1997). Modelling of a batch deep-fat frying process for tortilla chips. *Food and Bioproducts Processing 75*, 181-190. https://doi.org/10.1205/096030897531531

Estévez-Sánchez, K.H., Ruiz-Espinosa, H., Corona-Jiménez, E., López-Méndez, E.M., Cortés-Zavaleta, O., Ochoa-Velasco, C.E. and Ruiz-López, I.I. (2021). Water diffusivity estimation in air-dried complex-shaped foods by the method of slopes: application to oblate spheroid geometry. *Computers and Electronics in Agriculture 181*, 105949. https://doi.org/10.1016/j.compag.2020.105949

Ghaitaranpour, A., Mohebbi, M. and Koocheki, A. (2021). An innovative model for describing oil penetration into the doughnut crust during hot air frying. *Food Research International 147*, 110458. https://doi.org/10.1016/j.foodres.2021.110458

Gómez-de la Cruz, F.J., Palomar-Carnicero, J.M., Hernández-Escobedo, Q. and Cruz-Peragón, F. (2020). Determination of the drying rate and effective diffusivity coefficients during convective drying of two-phase olive mill waste at rotary dryers drying conditions for their application. *Renewable Energy 153*, 900-910. https://doi.org/10.1016/j.renene.2020.02.062

González-Pérez, J.E., López-Méndez, E.M., Luna-Guevara, J.J., Ruiz-Espinosa, H., Ochoa-Velasco, C. and Ruiz-López, I.I. (2019). Analysis of mass transfer and morphometric characteristics of white mushroom (*Agaricus bisporus*) pilei during osmotic dehydration. *Journal of Food Engineering 240*, 120-132. https://doi.org/10.1016/j.jfoodeng.2018.07.026

González-López, M.E., Laureano-Anzaldo, C.M., Pérez-Fonseca, A.A., Arellano and M., Robledo-Ortíz, J.R. (2021). A discussion on linear and non-linear forms of Thomas equation for fixed-bed adsorption column modeling. *Revista Mexicana de Ingeniería Química 20*, 875-884. https://doi.org/10.24275/rmiq/Fen2337

Gouyo, T., Goujot, D., Bohuon, P. and Courtois, F. (2021). Multi-compartment model for heat and mass transfer during the frying of frozen pre-fried French fries. *Journal of Food Engineering 305*, 110587. https://doi.org/10.1016/j.jfoodeng.2021.110587

Jeong, S., Kwak, J. and Lee, S. (2021). Machine learning workflow for the oil uptake prediction of rice flour in a batter-coated fried system. *Innovative Food Science and Emerging Technologies 74*, 102796. https://doi.org/10.1016/j.ifset.2021.102796

Kose, Y.E. and Dogan, I.S. (2017). Determination of simultaneous heat and mass transfer parameters of tulumba dessert during deep-fat frying. *Journal of Food Processing and Preservation 41*, e13082. https://doi.org/10.1111/jfpp.13082

Krokida, M.K., Oreopoulou, V. and Maroulis, Z.B. (2000a). Effect of frying conditions on shrinkage and porosity of fried potatoes. *Journal of Food Engineering 43*, 147-154. https://doi.org/10.1016/S0260-8774(99)00143-0

Krokida, M.K., Oreopoulou, V. and Maroulis, Z.B. (2000b). Water loss and oil uptake as a function of frying time. *Journal of Food Engineering 44*, 39-46. https://doi.org/10.1016/S0260-8774(99)00163-6

Li, P., Wu, G., Yang, D., Zhang, H., Qi, X., Jin, Q. and Wang, X. (2020). Analysis of quality

and microstructure of freshly potato strips fried with different oils. *LWT - Food Science and Technology 133*, 110038. https://doi.org/10.1016/j.lwt.2020.110038

Movahhed, S. and Chernabon, H.A. (2019). Moisture content and oil uptake variations and modeling in deep-fat frying hamburger slices. *Chemical Product and Process Modeling 14*, 20180036. https://doi.org/10.1515/cppm-2018-0036

Moyano, P.C. and Berna, A.Z. (2002). Modeling water loss during frying of potato strips: effect of solute impregnation. *Drying Technology 20*, 1303-1318. https://doi.org/10.1081/DRT-120005854

Naghavi, E.-A., Dehghannya, J. and Ghanbarzadeh, B. (2018a). 3D computational simulation for the prediction of coupled momentum, heat and mass transfer during deep-fat frying of potato strips coated with different concentrations of alginate. *Journal of Food Engineering 235*, 64-78. https://doi.org/10.1016/j.jfoodeng.2018.04.026

Naghavi, E.-A., Dehghannya, J. and Ghanbarzadeh, B. (2018b). Effect of hydrocolloid type on transfer phenomena during deep-fat frying of coated potato strips: numerical modeling and experimental analysis. *Computers and Electronics in Agriculture 154*, 382-399. https://doi.org/10.1016/j.compag.2018.09.024

Nikolau, M. (2006). Control of snack food manufacturing systems. *IEEE Control Systems Magazine 26*, 40-53. https://doi.org/10.1109/MCS.2006.1657875

Olguín. J.A., Vazquez-León, L.A., Salgado-Cervantes, M.A., Fernández-Barbero, G., Díaz-Pacheco, A., García-Alvarado, M.A. and Rodríguez-Jimenes, G.C. (2019). Water and phytochemicals dynamic during drying of red habanero chili pepper (*Capsicum chinense*) slices. *Revista Mexicana de Ingeniería Química 18*, 851-864. https://doi.org/10.24275/uam/izt/dcbi/revmexingquim/2019v18n3/Olguin

Ortiz-García-Carrasco, B., Yañez-Mota, E., Pacheco-Aguirre, F.M., Ruiz-Espinoza, H., García-Alvarado, M.A., Cortés-Zavaleta, O. and Ruiz-López, I.I. (2015). Drying of shrinkable food products: Appraisal of deformation behavior and moisture diffusivity estimation under isotropic shrinkage. *Journal of Food Engineering 144*, 138-147. https://doi.org/10.1016/j.jfoodeng.2014.07.022

Ramachandran, R.P., Paliwal, J. and Cenkowski, S. (2018). Modeling effective moisture diffusivity and activation energy of distillers' spent grain pellets with solubles during superheated steam drying. *Biomass and Bioenergy 116*, 39-48. https://doi.org/10.1016/j.biombioe.2018.06.004

Rice, P. and Gamble, M.H. (1989). Technical note: modelling moisture loss during potato slice frying. International *Journal of Food Science and Technology 24*, 183-187. https://doi.org/10.1111/j.1365-2621.1989.tb00632.x

Roshani, F., Movahhed, S. and H.A. Chenarbon. (2021). Modelling shrinkage in deep-fried satina potato slices pretreated with ultrasound. *Potato Research 64*, 257-265. https://doi.org/10.1007/s11540-020-09475-9

Topete-Betancourt, A., Figueroa-Cárdenas, J.D.J., Morales-Sánchez, E., Arámbula-Villa, G. and Pérez-Robles, J.F. (2020). Evaluation of the mechanism of oil uptake and water loss during deep-fat frying of tortilla chips. *Revista Mexicana de Ingeniería Química 19*, 409-422. https://doi.org/10.24275/rmiq/Alim605

Tlatelpa-Becerro, A., Rico-Martínez, R., Urquiza, G. and Calderón-Martínez, M. (2020). Obtaining of Crataegus mexicana leaflets using an indirect solar dryer. *Revista Mexicana de Ingeniería Química 19*, 669-676. https://doi.org/10.24275/rmiq/Alim896

Touffet, M., Trystam, G. and Vitrac. O. (2020). Revisiting the mechanisms of oil uptake during deep-frying. *Food and Bioproducts Processing 123*, 14-30. https://doi.org/10.1016/j.fbp.2020.06.007

Wu, H., Karayiannis, T.G. and Tassou, S.A. (2013). A two-dimensional frying model for the investigation and optimization of continuous industrial frying systems. *Applied Thermal*

Engineering 51, 926-936. https://doi.org/10.1016/j.applthermaleng.2012.10.002

Yildiz, A., Palazoğlu, T.K. and Erdoğdu, F. (2007). Determination of heat and mass transfer parameters during frying of potato slices. *Journal of Food Engineering 79*, 11-17. https://doi.org/10.1016/j.jfoodeng.2006.01.021

Ziaiifar, A.M., Courtois, F. and Trystam, G. (2010). Porosity development and its effect on oil uptake during frying process. *Journal of Food Process Engineering 33*, 191-212. https://doi.org/10.1111/j.1745-4530.2008.00267.x